J Therm Anal Calorim (2014) 115:177–183
DOI 10.1007/s10973-013-3245-6

Comparison of solar silicon feedstock

Aleksandar M. Mitrašinović · Francisco C. Robles Hernández

Received: 30 July 2012 / Accepted: 7 May 2013 / Published online: 7 June 2013

Abstract One of the major factors in reducing a cost of commercial solar cells is the lifetime of the photovoltaic material. In this work, a deterioration of Si generated by solvent metal gathering method (SMG) and Si removed from damaged solar cells is analyzed and compared with electronic grade Si. The differences in heating and cooling cycles on the DTA curves of different solar grade Si and Cu–Si mixtures are compared. A nonequilibrium exothermic reaction in Si generated by SMG method is recorded in samples aged in room atmosphere for 1 year. The outcomes of the cooling cycles after the DTA analyses for various solar grades Si were not significantly differentiated from the referred electronic grade Si indicating that recrystallization of aged Si diminishes the problem related to agglomeration of Cu and oxygen on the surface of Si solar grade particles. The DTA tests showed that recrystallized Si from the deteriorated solar cells can be recycled as feedstock materials for solar cells applications while Si generated by SMG method can be used for blending in order to achieve a long lifetime of Si solar cells.

A. M. Mitrašinović (✉)
Centre for Advanced Coating Technologies, University of Toronto, Bahen Centre for Information Technologies, Rm 8268, 40 St. George St, Toronto, ON M5S 3G8, Canada
e-mail: alex.mitrasinovic@utoronto.ca

A. M. Mitrašinović
Department of Materials Science and Engineering, 184 College St, Mining Bldng, Room 208, Toronto, ON M5S 3E4, Canada

F. C. Robles Hernández
Mechanical Engineering Technology, University of Houston, 304A Technology Building, Houston, TX 77204-4020, USA

Keywords Solar Si · Surface impurities · Si deterioration · Si recyclability

Introduction

Traditionally, silicon used for photovoltaic applications were supplied from the same feedstock like the electronic industry. With the recent steep increase in demand for solar grade silicon, silicon produced by chemical vapor deposition is above the required quality for photovoltaic applications but its production cost is high for large-scale production of solar cells [1]. Consequently, a large amount of silicon produced by different techniques is introduced into photovoltaic market [2, 3]. Researchers estimated that in a few decades with price increases and possible depletion of traditional sources of energy implementation of the affordable and low energy demanding techniques in solar grade silicon production, solar power can evolve into a major source of energy [4].

One of the methods for refining silicon that can achieve a solar grade quality is adding a solvent metal with higher affinity to impurities in silicon produced by carbothermic process [5, 6]. The solvent metal, besides being capable of gathering the impurities has to be easily removable from the silicon in the last step of refining. Al has been successfully used as a solvent metal where the significant difference in melting temperatures between Al and Si was utilized [7, 8]. Cu has a considerably lower melting temperature than Si but more importantly has a significantly higher density than Si. Low solid solubility of Cu in Si [9] and high diffusion coefficient of interstitial Cu^{+} ions in Si crystal [10] further favor utilization of the solvent metal gathering method (SMG) in silicon refining process where Cu is the solvent element [11, 12]. Since more work has to

be done in order to achieve consistent quality of SolSi generated by SMG method, in practical applications, many producers of inexpensive solar grade Si are blending Si rejected from electronic industry with recycled solar Si and Si refined using one of the emerging technologies [13–15]. With increased number of new technologies for solar Si production, new methods for characterization of feedstock Si material using e.g., scanning near-field optical microscope [16], thermogravimetry in series with Fourier transform infrared spectroscopy [17], or microscopy and gravimetric analyses [18] can be suggested similarly to characterization of the other photovoltaic material [19].

Implementation of simple and widely available technique such as differential thermal analysis (DTA) for quality control of input material can significantly reduce the overall production cost of SolSi and the amount of rejected material. The aim of this work is to compare properties of electronic grade, recycled solar grade silicon and solar grade silicon produced by SMG method and to assess the long-term effect of the solvent element on solar grade silicon. DTA technique was used to determine the thermochemical properties of input material with a different origin and purity and obtained results were correlated to photovoltaic properties of produced SolSi.

Quality control in SolSi production by SMG method

The quality control of the SolSi production process relies on advanced trace elements techniques such as inductively coupled plasma mass spectrometry (ICP–MS), neutron activation analysis (NAA), atomic absorption spectrometry (AAS), or glow discharge mass spectrometry (GDMS). Although all techniques have sensitivity below 1 ppm for most elements, an accurate assessment of entire sample requires large number of measurement. Figure 1 shows typical process steps in the SolSi production with the quality control test stations positions. The last control station includes additional resistivity test or/and conversion efficiency assessment which is sometimes due to the special requirements of advanced analytical techniques only one applied quality control test. In the high capacity processes utilizing low operational demands and low-cost input material, maintenance cost of analytical testing equipment and requirements for highly qualified personnel can noticeably increase an overall cost of the final product. Providing accurate quality control model based on the standard characterization technique at the early stage of SolSi production can significantly reduce production cost and prevent large amount of rejected material after the final steps of production. The correlation between characteristic points on DTA curves and quality of the final product can give reliable data for assessment of input material in SolSi production process.

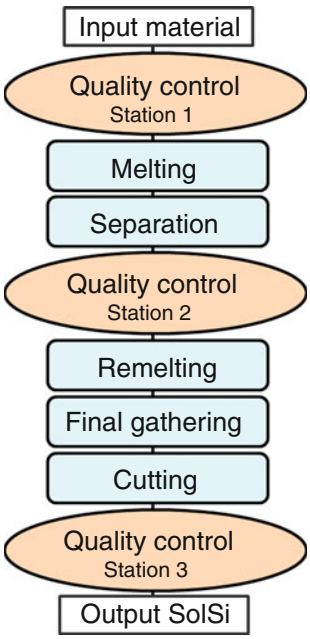

Fig. 1 Typical process steps in SolSi production by SMG method with quality control test stations positions

Materials selection and testing procedure

Four samples with 50, 30, 17, and 13 %Si chemical composition (rest is Cu) were analyzed immediately after mixing and 1 year later (aged samples). The composition and mass of the different grade Si samples and Cu–Si mixture used in this work are given in Table 1. Two Cu–Si mixtures, 50 and 30 %Si, were approximately matching 1–2 and 1–1 atomic ratio between Cu and Si. 17 %Si is the eutectic composition for the Cu–Si system on the side where the pure Si phase is formed while 13 %Si corresponds to the maximum of the congruent transformation between two eutectics, which also corresponds closely to single Cu_3Si phase at room temperature. Also, silicon plates removed from Ontario's solar cells ($SolSi_{Recycled}$) due to short circuits or burnings and solar grade silicon generated by SMG method ($SolSi_{SMG}$) were analyzed by DTA technique. Electronic Si (EgSi) was used for comparing and calibration purposes.

Cu–Si mixture samples were prepared by mixing EgSi and electrolytic grade Cu in mullite crucibles and melted at 1,500 °C in Lindberg furnace. After solidifying, the Cu–Si samples were 3 cm in height with 2.54 cm diameter. All samples indicated in Table 1 were crushed into 100 ± 20 μm particles size. Approximately 100 mg of each sample was used immediately for DTA. The remaining sample was aged in the room atmosphere and analyzed under the same conditions 1 year later.

The unit used for DTA tests is a SETARAM 92-16.18 DTA/TGA analyzer. The vessels with reference alumina

Table 1 Mass of the DTA samples and mullite crucibles

Sample Id	Vessel/mg	Al_2O_3/mg	Mixture/mg
EgSi	255	100	100
$SolSi_{Recycled}$	256	100	100
$SolSi_{SMG}$	256	100	100
50Si	256	100	97
30Si	254	100	99
17Si	256	100	103
13Si	256	100	98
$SolSi_{SMG}$ (aged)	241	120	119
50Si (aged)	238	120	126
30Si (aged)	238	120	126
17Si (aged)	243	120	121

Sample Id indicates amount of silicon in mass percent while the rest is copper

powder and investigated sample were placed on the sample holders. Two thermocouples were placed beneath the vessels. The stand with the vessels was lowered into the analyzer chamber. The chamber was evacuated and filled with argon gas to create an inert atmosphere. The gas flow rate of 100 mL min^{-1} was kept constant. All DTA measurements were set to begin and end at 400 °C with maximum temperature of 1,450 °C. The sensitivity range for the B-type thermocouple is from 500 °C up to 1,800 °C. Due to wide range of temperature a relatively high heating and cooling rate of 15 °C min^{-1} was used in all tests. The SETARAM CS92 temperature controller monitored the temperature while the results were recorded with frequency of heat flow readings of one per minute. Extrapolation method [20] by ASTM E794 standard was used in all instances to determine the characteristic temperatures at the DTA curves.

The Raman characterization was done on a confocal micro-Raman microscope XploRA^{TM}, Horiba JY. The lasers used for the Raman excitation include the following wave lengths: 532 and 638 nm. The $SolSi_{SMG}$ and 50Si samples were investigated and the results are presented in normalized intensity to enhance the mean features and characteristics.

Comparison of DTA analyses for EgSi and SolSi with various origin

Figure 2 shows the DTA curves for the different types of solar grade Si. For pure Si, only one peak should be recognized at 1,414 °C. The recorded freezing temperatures around 1,400 °C are due to relatively high cooling rate of 15 °C min^{-1}. Furthermore, at high temperature the DTA chambers release heat at a lower rate than that is set up which further decrease readings for the freezing point of Si during the DTA tests. $SolSi_{Recycled}$ sample did not show any reaction besides melting and did not differentiate from the referred EgSi. $SolSi_{SMG}$ sample had the same characteristic temperatures like EgSi with slight difference in the DTA curve in 1,380–1,410 °C temperature range and unforeseen exothermic reaction at 1,035 °C during heating cycle for aged sample.

The influence of Cu as major gathering element and its catalytic properties on exothermic reaction in $SolSi_{SMG}$ sample can be examined by analyzing mixtures with different amounts of Cu in Si. The DTA curves for four tests carried out for samples with various amounts of Cu and Si with respect to temperature are shown in Fig. 3. The first transformation during heating is recognized at 540 °C where Cu_3Si intermetallic has a lattice transformation in solid. All Cu–Si mixtures showed distinctive eutectic reactions at around 790 °C which correlate to melting of the Cu_3Si microconstituent where the higher peaks and increased area below peaks refer to higher enthalpy of corresponding transformation. The 50Si mixture revealed liquidus transformation at around 1,200 °C. Table 2 shows characteristic temperatures for SolSi and Cu–Si mixtures during heating and cooling cycle. The results given in

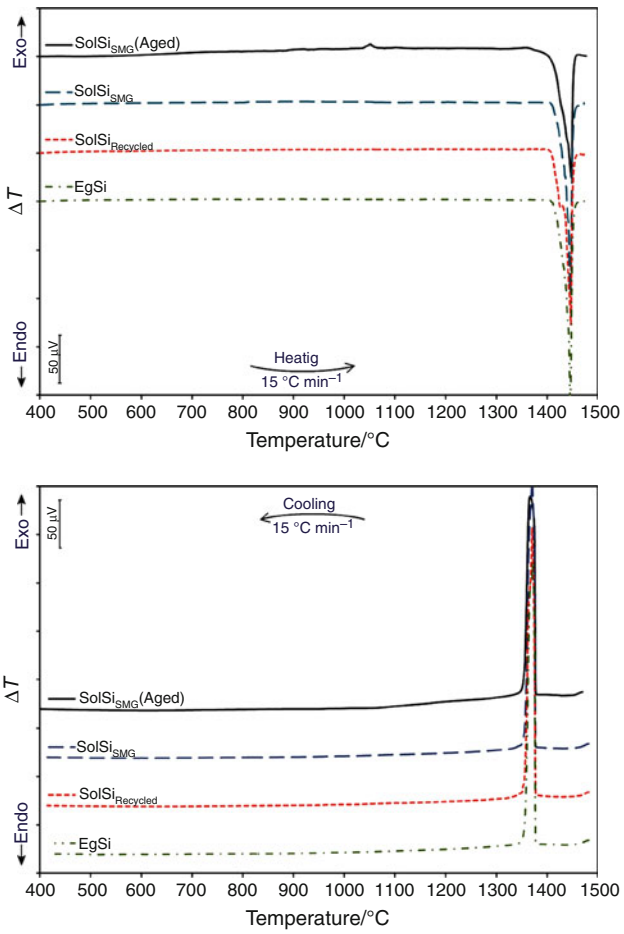

Fig. 2 Characteristic DTA *curves* for different high purity Si

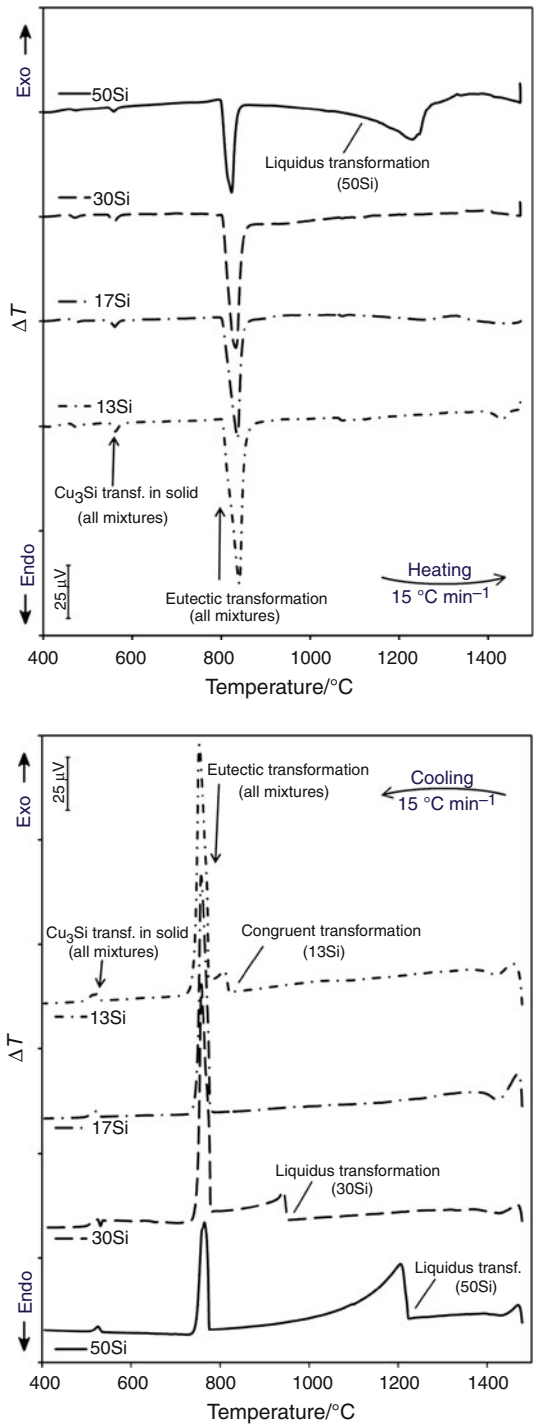

Fig. 3 DTA *curves* as function of temperature during heating and cooling for four Cu–Si mixtures

Table 2 are for different Cu and Si compositions that were obtained immediately after the mixtures formed.

During the heating cycle, the eutectic transformation is observed in both 50Si and 30Si mixtures. The liquidus transformation is clearly revealed for 50Si while the 30Si mixture has a slight displacement from the baseline without distinguishable peak. During the cooling cycle both

Table 2 Characteristic transformation temperatures in °C for SolSi samples and Cu–Si mixtures

	Transf. in Solid	Eutectic	Liquidus/melting
Heating cycle			
EgSi	–	–	1405 (1445)
$SolSi_{Recycled}$	–	–	1400 (1445)
$SolSi_{SMG}$	–	–	1400 (1445)
50Si	540 (550)	790 (820)	n/a (1235)
30Si	540 (555)	790 (830)	n/a
17Si	540 (555)	790 (835)	–
13Si	540 (555)	790 (840)	n/a
Cooling cycle			
EgSi	–	–	1390 (1375)
$SolSi_{Recycled}$	–	–	1385 (1375)
$SolSi_{SMG}$	–	–	1385 (1375)
50Si	540 (530)	785 (770)	1235 (1210)
30Si	540 (530)	780 (760)	960 (945)
17Si	540 (530)	775 (755)	–
13Si	540 (530)	n/a (755)	830 (810)

The peak temperatures of the corresponding transformation are given in brackets. n/a refers to inconclusive temperature of existing transformation

transformations, liquidus and solidus are recognized in 50Si and 30Si mixtures.

During the heating cycle in mixtures close to eutectic composition (30Si, 17Si, and 13Si) only the eutectic transformation is observed. Cu–Si mixture samples were completely melted at the eutectic temperature and liquidus or congruent transformations did not occur. During the cooling cycle, the liquidus transformation is found for the 30Si mixture while the 17Si mixture did not show any transformation until the eutectic. The peak of the curve at 810 °C for 13Si mixture corresponds to the congruent transformation.

DTA analyses of the aged SolSi and Cu–Si mixtures

To understand better possible deterioration effects on the surface microstructure of the $SolSi_{SMG}$ material, DTA analysis of samples aged for 1 year were conducted (Fig. 4). Characteristic transformation temperatures for samples generated immediately after mixing (Fig. 3) are closer to equilibrium conditions and simple to detect and characterize than matching samples generated 1 year later (Fig. 4). The DTA curves of the solar grade silicon had almost straight shape. Among SolSi samples only $SolSi_{Alloy}$(aged) had an exothermic reaction at 1,035 °C. Similar exothermic reaction at the same temperature is registered for all Cu–Si aged samples.

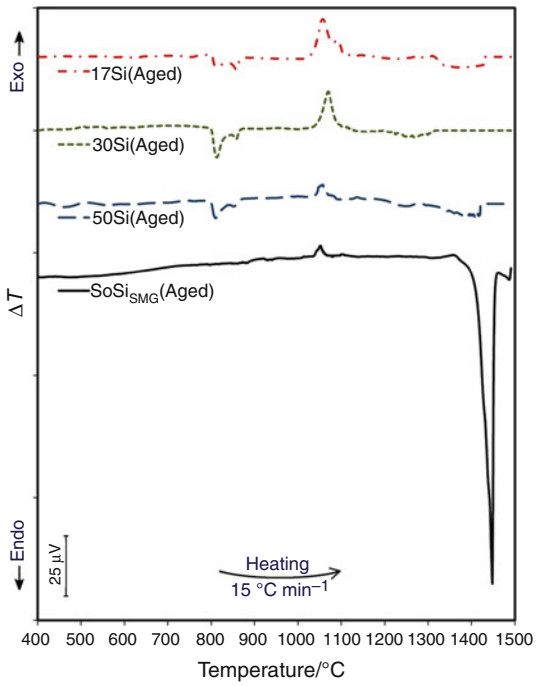

Fig. 4 DTA *curves* as function of temperature during heating for aged samples

During heating, eutectic transformation for a 50Si mixture has a lower peak and smaller area below the peak in comparison to matching the aged sample. An indistinguishable liquidus temperature during heating cycle in Fig. 3 for 50Si aged sample indicated the presence of inhibiting layer on the surface of the aged particles. 17Si sample in Fig. 4 had similar eutectic transformation behavior like the 50Si samples but with a significantly higher peak and area below. However, an exothermic reaction is recognized at 1,035 °C that indicates existence of the complex reaction on the surface between silicon, copper, and oxygen resulting in the formation of Si–Cu–O compounds. Similar phenomenon is recently recognized in glass system where P–O–Cu intermediate complex is formed [21]. The existence of the nonequilibrium liquidus transformation in aged 17Si sample during heating suggests that Cu was consumed for exothermic reaction at 1,035 °C. However, during cooling the liquidus is not recorded which indicated complete decomposition of the Cu–Si–O compounds. The summarized characteristic transformation temperatures identified during the heating cycles and cooling cycles of the aged samples are given in Table 3.

Exothermic reaction in aged solar grade silicon originated by SMG method

Outcomes from the DTA analyses for the aged SolSi samples indicated the existence of chemically active trace elements at high temperatures. Surface of the SolSi particles was covered with a thin layer of silicon and impurity oxides whose fine dispersion along the surface had recognizable effect on the DTA curves shape. During the heating, an exothermic reaction is recognized around 1,035 °C that indicates a complex reaction between Si, Cu, and oxygen resulting in formation of Si–Cu oxides.

The liquidus temperature during heating could not be clearly deducted in Fig. 4 for aged 50Si sample due to the presence of fine Si–Cu oxides at the surface of silicon particles while the liquidus transformation is distinguished at 1,240 °C during cooling. Another indication of the chemically active Si particles surface is the explicit eutectic reaction at 795 °C but a jagged curve from the solidus up to liquidus for aged 50Si sample in Fig. 4. The obtained results reveal the existence of a complex system rather than a simple two-component system. The exothermic reactions detected at temperatures between 1,030 and 1,035 °C most likely correspond to a reaction between melting of the copper oxides and its reaction with silicon forming elemental copper and silicon oxide. Although due to low amount of Cu and Oxygen a Si-rich silicide and

Table 3 Characteristic temperatures in °C during heating for aged solar grade Si and Cu–Si mixture particles

	Transf. in solid	Eutectic	Cu–Si–O	Liquidus/melting
Heating cycle				
SolSi$_{SMG}$ (aged)	–	–	1,030 (1045)	1,390 (1450)
50Si (aged)	n/a (500)	795 (805)	1,035 (1055)	n/a (1410)
30Si (aged)	n/a (495)	795 (810)	1,035 (1170)	1,220 (1265)
17Si (aged)	n/a	795 (810)	1,030 (1060)	1,305 (1340)
Cooling cycle				
SolSi$_{SMG}$ (aged)	–	–	–	1,385 (1375)
50Si (aged)	540 (530)	780 (770)	–	1,240 (1215)
30Si (aged)	540 (530)	775 (765)	–	980 (955)
17Si (aged)	540 (530)	775 (765)	–	–

n/a refers to inconclusive temperature of existing transformation

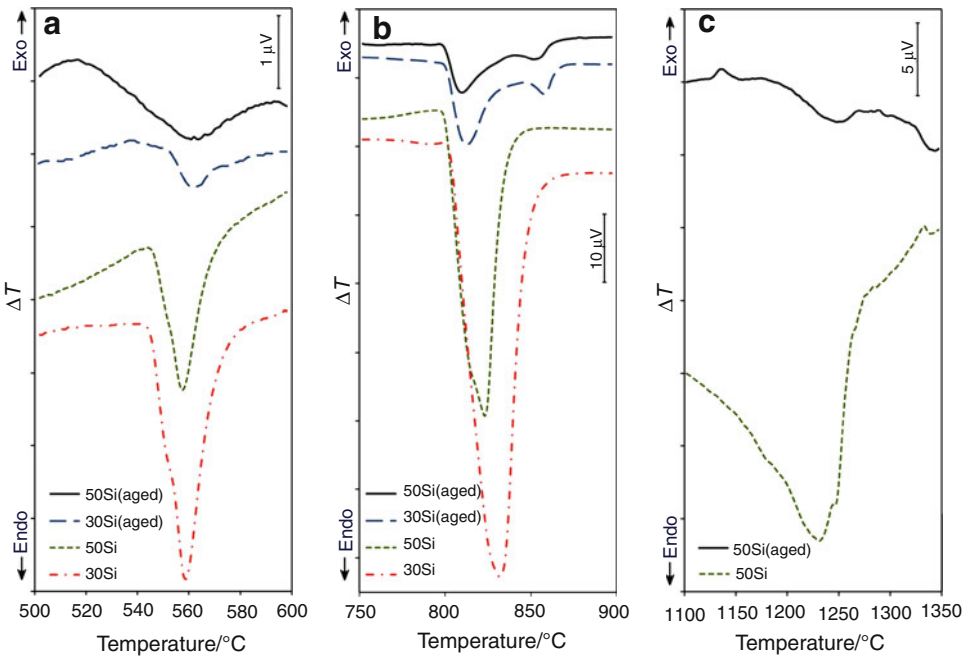

Fig. 5 Difference in the DTA *curves* for aged and non-aged Cu–Si mixtures during heating cycle. **a** Transformation in solid, **b** solidus and **c** liquidus

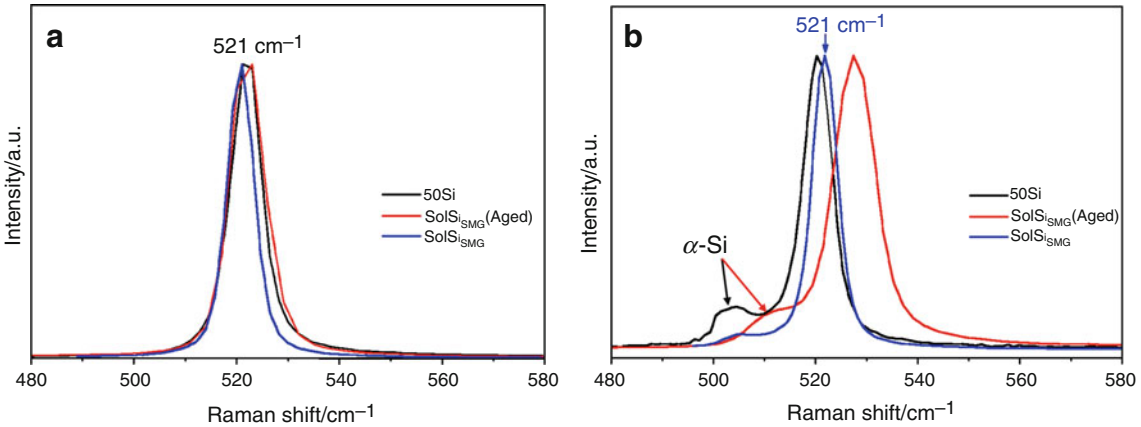

Fig. 6 Raman spectra for the pure silicon and Cu–Si mixture samples for **a** 532 nm and **b** 638 nm laser excitation

oxides are formed, the detected transformation in the simplest form can be explained by $2\ Cu_2O + Si = 4\ Cu + SiO_2$ chemical reaction. High Cu diffusion in Si lattice makes Cu atoms gather at the surface of Si particles and together with absorbed oxygen instigating nonequilibrium exothermic reaction at 1,035 °C.

The differences between aged and non-aged samples are more pronounced for heating than for the cooling cycle. Figure 5 shows an effect of aging and emphasizes that different shapes of the DTA curves originated immediately after mixing and after aging. The transformation in the solid at 540 °C is not clear in the aged samples while in non-aged samples the solid transformation of the Cu_3Si is clearly recognized (Fig. 5a). Both mixtures, 50Si and 30Si are hypereutectic meaning that they should have two characteristic transformations at solidus and liquidus temperatures. Although all samples have the same solidus temperature, the non-aged samples have a larger area below the solidus peak (Fig. 5b). The largest difference in DTA curves is observed in the liquidus region during heating (Fig. 5c). Liquidus transformations during heating occur at the range of temperatures in aged samples, while during cooling the liquidus temperature is easy to determine.

Raman spectra in the SolSi and Cu–Si mixtures

Figure 6 shows two Raman spectra for the pure silicon and Cu–Si mixture samples. The Raman shift for silicon is constant for unstressed silicon; however, it is quite

sensitive to residual stresses [22]. Peaks at $\sim$521 cm^{-1} in Fig. 6a show highly crystalline species [23] indicating that the investigated pure silicon sites are stress-free regions. In Fig. 6b spectra using a 638 nm laser of the Cu–Si regions in Cu–Si mixture sample are presented. Two main characteristics can be identified in those spectra: (i) the second peak that is likely related to the α-Si is known as amorphous silicon [24] and (ii) the shift in the Raman peak from 521 cm^{-1}. This shift is an indication of residual stresses in the sample. Therefore, existence of the shift in Raman peaks in SolSi sample can be indication of its deterioration while fractions of α-Si can be used to assess the percentage of amorphous phase.

Conclusions

A set of analysis was performed on input material for SolSi production and various SolSi material originated by different techniques in order to investigate the aging effect on various SolSi material. In a long time period only SolSi produced by SMG method showed significant change in properties important for photovoltaic applications. Results showed that the DTA technique can be used for initial quality assessment of SolSi material before proceeding to other advanced analytical and characterization techniques. Also, DTA technique is capable of detecting agglomerated Cu at the surface of SolSi particles generated by SMG method. Recrystallized Si from the deteriorated solar cells can be recycled and used as feedstock materials for solar cells applications. The outcomes of the cooling cycles after the DTA analyses for various SolSi grades did not differentiate from the referred electronic grade Si indicating that recrystallization of aged Si diminishes the problem related to agglomeration of excessive Cu and Oxygen on the surface of SolSi generated by SMG method. However, comparison of different Si–Cu mixtures indicated that Cu acts as a catalyst for surface oxidation which can reduce conversion efficiency and, therefore, such material is recommended for use in blending with SolSi with lower Cu concentration.

References

1. Jester T. Crystalline silicon manufacturing progress. Prog Photovolt. 2002;10:99–106.
2. Genieva S, Turmanova S, Dimitrova A, Vlaev L. Thermal degradation of rice husks and characterization of the products. J Therm Anal Calorim. 2008;93:387–96.
3. Gu J, Fahrenkrug E, Maldonado S. Direct electrodeposition of crystalline silicon at low temperatures. J Am Chem Soc. 2013; 135:1684–87.
4. Mitrašinović A. Photo-catalytic properties of silicon and its future in photovoltaic applications. Renew Sustain Energy Rev. 2011;15:3603–7.
5. Abdyukhanov I, Abdyukhanov M, Kuz'min Y, Merkushkin V. Production of metallurgical silicon of enhanced quality for land-based solar cells. Met Sci Heat Treat. 2000;42:246–9.
6. Arkhipov M, Dubovskiy A, Reu A, Mukhanov V, Smirnova S. Carbothermic synthesis of silicon in 150 kW DC arc furnace for solar applications. Silicon for the Chem and Sol Ind. IX, Oslo, Norway, 2008.
7. Yoshikawa T, Morita K. Refining of silicon during its solidification from a Si–Al melt. J Cryst Growth. 2009;311:776–9.
8. Gumaste J, Mohanty B, Galgali R, Syamaprasad U, Nayak B, Singh S, Jena P. Solvent refining of metallurgical grade silicon. Sol Energy Mater. 1987;16:289–96.
9. Olesinski R, Abbaschian G. The copper–silicon system. Bull of Alloy Phase Diagr. 1986;7:170–8.
10. Buonassisi T, Marcus M, Istratov A, Heuer M, Ciszek T, Lai B, Cai Z, Weber E. Analysis of copper-rich precipitates in silicon: chemical state, gettering, and impact on multicrystalline silicon solar cell material. J Appl Phys. 2005;97:063503.
11. Mitrašinović A, Utigard T. Trace elements distribution in Cu–Si alloys. Chem Phys Lett. 2011;515:72–7.
12. Mitrašinović A, Utigard T. Copper removal from hypereutectic Cu–si alloys by heavy liquid media separation. Metall Mater Trans B. 2012;43:379–87.
13. Bronsveld P, Naber R, Geerligs L, Pozigun S, Syvertsen M, Knopf C, Kvande R. p and n-type mono and mc-Si solar cells using blended upgraded metallurgical grade silicon. 24th European Photovoltaic Solar Energy Conference and Exhibition 2009 21–25 September, Hamburg, Germany.
14. Pavone A. Polysilicon for solar wafers. SRI Consulting, Process Econ Progr. PEP Report No.272, December 2009.
15. Mitrašinović A, D'Souza R, Utigard T. Impurity removal and overall rate constant during low pressure treatment of liquid silicon. J Mater Process Technol. 2012;212:78–82.
16. Grmela L, Škarvada P, Tománek P, Macků R, Smith S. Local investigation of thermal dependence of light emission from reverse-biased monocrystalline silicon solar cells. Sol Energy Mater & Sol Cells. 2012;96:108–11.
17. Miller T. Use of TG/FT-IR in material characterization. J Therm Anal Calorim. 2011;106:249–54.
18. Ould-Abbas A, Bouchaour M, Trari D, Chabane Sari N. The impact of drying phenomena and heat treatment on the structure of porous silicon. J Therm Anal Calorim. 2012;109:1347–51.
19. Madarász J, Nagygyörgy V, Stathatos E, Pokol G. Ageing and thermal stability studies on quasi-solid composite electrolytes for Grätzel-type solar cells. J Therm Anal Calorim. 2013;. doi: 10.1007/s10973-012-2904-3.
20. Boettinger W, Kattner U, Moon K, Perepezko DTA and Heat-flux DSC Measurements of Alloy Melting and Freezing. J Natl Inst Stand Technol. 2006 Special Publication 960-15, U.S. Department of Commerce.
21. Sułowska J, Wacławska I, Szumera M. Effect of copper addition on glass transition of silicate–phosphate glasses. J Therm Anal Calorim. 2012;109:705–10.
22. DeWolf I. Micro-Raman spectroscopy to study local mechanical stress in silicon integrated circuits. Semicond Sci Tech. 1996;11:139–54.
23. Robles Hernandez F, De Cruz Rivera. Micro-Raman analysis of the Si particles present in Al–Si hypereutectic alloys in liquid and semi-solid states. J Adv Eng Mater. 2007;9:46–51.
24. Schade M, Varlamova O, Reif J, Blumtritt H, Erfurth W, Leipner H. High-resolution investigations of ripple structures formed by femtosecond laser irradiation of silicon. Anal Bioanal Chem. 2010;396:1905–11.